Macromolecules **1993,** *26,* 5118–5124

Linear Multiblock Copolymer/Homopolymer Blends of Constant Composition. 1. Low-Molecular-Weight Homopolymers

Richard J. Spontak,* Steven D. Smith, and Arman Ashraf

Miami Valley Laboratories, The Procter & Gamble Company, Cincinnati, Ohio 45239-8707

Received October 6, 1992; Revised Manuscript Received May 27, 1993

ABSTRACT: Bicontinuous morphologies constitute an exciting new genre of microstructure in microphase-separated block copolymers and have thus far been observed in neat poly(styrene-*b*-isoprene) (SI) diblock and star-block copolymers, as well as in binary copolymer/homopolymer and copolymer/copolymer blends. While diblock and star-block copolymers differ in their molecular architectures, they both possess terminal (outer) blocks composed of a single monomer species. These terminal blocks are anchored at one end (the block junction) and unconstrained at the other. In the present work, linear $(SI)_n$ multiblock copolymers which consist of n ($2 \leq n \leq 4$) perfectly-alternating SI block pairs are blended with homopolystyrene (hPS). The conditions under which these blends are prepared are identical to those used to generate the ordered bicontinuous double-diamond (OBDD) morphology in $(SI)_1$/hPS blends. Transmission electron microscopy (TEM) reveals, however, that none of the blends produced here exhibit this morphology. In some cases, hPS is solubilized within the copolymer microstructure, resulting in either dispersed isoprene cylinders or swollen lamellae. Macrophase separation also occurs, depending on copolymer architecture and block length. The morphologies observed in this work are interpreted in terms of the conformational behavior of linear multiblock copolymers and competition between microphase ordering and macrophase separation.

Introduction

Modified and bicontinuous morphologies in microphase-separated block copolymers have recently become a subject of considerable interest. The bicontinuous morphology most extensively studied thus far is the ordered bicontinuous double-diamond (OBDD),[1,2] an example of which is presented in Figure 1. It belongs to the *Pn*3*m* space group[3] and can be generated in neat poly(styrene-*b*-isoprene) (SI) diblock[1] and star-block[2] copolymers when the volume fraction of the styrene block lies between 62 and 66 vol %. Transmission electron microscopy (TEM) studies[4–6] have shown that the styrene-rich version of this morphology (i.e., styrene matrix with isoprene channels) can also be produced in blends of SI diblock copolymers and polystyrene homopolymers (hPS) when (i) the total styrene composition (Φ_S) is about 65–67 vol %, (ii) the molecular weight of the hPS is less than that of the styrene block in the copolymer, (iii) the molecular weight of the hPS is near or below its critical molecular weight of entanglement (≈36 000), and (iv) the blend is prepared under conditions sufficiently far from the order–disorder transition (ODT). In addition, the OBDD morphology has been observed[7] in binary blends of two microphase-separated SI copolymers of identical molecular weight but different compositions when $\Phi_S \approx 0.61$.

Thomas and co-workers[3,8,9] have been successful in elucidating the geometric properties of various block copolymer morphologies, including the OBDD, by relating them to periodic area-minimizing surfaces of constant mean curvature. This approach is analogous to that taken by Anderson et al.[10] to identify organized structures produced by small-molecule amphiphiles, which, when mixed with oil and water, tend to undergo self-assembly into similarly ordered morphologies. While these efforts have provided tremendous insight into the structural aspects of complex three-dimensional morphologies, the phase stability of bicontinuous morphologies in microphase-separated diblock copolymers remains poorly understood.[11] Wang and Safran[12] have shown that it is dependent on free-energy considerations such as the curvature elastic moduli, and Winey et al.[4,5] have demonstrated that it is further complicated in copolymer/homopolymer blends by both the spatial distribution of homopolymer solubilized within its preferred microdomain and the area density of junction sites within the microdomain-separating interphase.

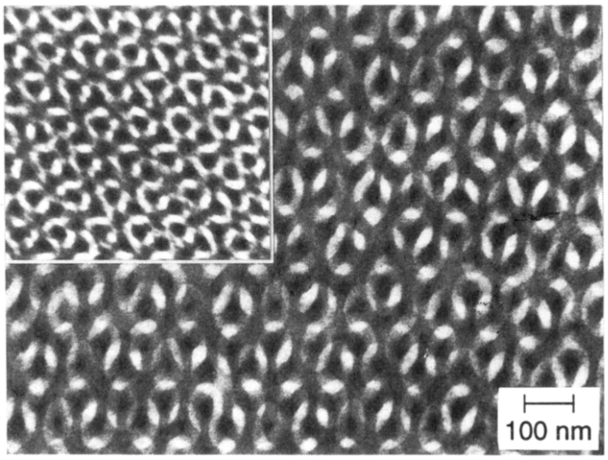

Figure 1. Energy-filtered electron micrograph of the ordered bicontinuous double-diamond (OBDD) morphology produced in a blend composed of a symmetric SI diblock copolymer and hPS at 66 vol % styrene. The copolymer block weights are 30 000 each, whereas the molecular weight of hPS is 15 000. The image shown in the inset (enlarged by 1.6×) is obtained from a 15 000/15 000 SI copolymer and hPS3. They both clearly illustrate the "wagon-wheel" projection along the [111] axis.

Another factor to be considered in forming a bicontinuous morphology is the molecular architecture of the copolymer, since it regulates the various chain conformations which are possible (see Figure 2). In the case of the simple diblock architecture, each block is anchored at one end (the junction site) and free at the other, and the number of junction sites within an interphase is equal to the number of molecules occupying the interphase. Two-component *m*-arm star-block copolymers are designed much in the same way as symmetric triblock copolymers and consist of *m* terminal (outer) blocks which are free at one end, along with *m* middle blocks which are constrained

---

* To whom correspondence should be addressed at the Department of Materials Science and Engineering, North Carolina State University, Raleigh, NC 27695.

0024-9297/93/2226-5118$04.00/0

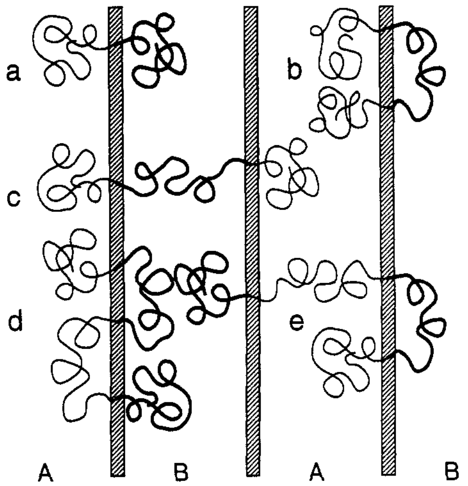

Figure 2. Schematic diagram of linear A/B block copolymers possessing different architectures in a lamellar morphology. The AB diblock copolymer ($n = 1$) is presented as (a), followed by symmetric ABA triblock copolymers (b,c). Triblock (and star-block) copolymers are capable of looping back upon themselves (b) or bridging a microdomain core (c). An $(AB)_2$ tetrablock copolymer can assume four different conformations upon microphase separation: one fully looped (d), one fully bridged (not displayed here), and two in which one middle block is looped and the other bridged (e). At equilibrium, each block junction in these molecules must reside within an interphase region (cross-hatched).

at both ends. In the case of star-block and triblock copolymers, the number of junction sites per molecule per interphase is either one or two, depending on molecular conformation.

Linear poly(styrene-*b*-isoprene)$_n$ $(SI)_n$ multiblock copolymers are more complex in terms of the numerous conformations they may adopt.[13-15] Symmetric molecules are composed of $2n$ perfectly-alternating styrene and isoprene blocks and possess $n - 1$ middle S blocks and $n - 1$ middle I blocks for a total of $2(n - 1)$ middle blocks, all of which are anchored at both ends and fully constrained in microdomain space. Only the two terminal blocks possess a free end. Thus, unlike diblock and star-block copolymers (which can order into the OBDD morphology), $(SI)_n$ copolymers with $n > 1$ consist of *both* constrained and free-ended S and I blocks, the ratio of which depends explicitly on n. The total number of different conformations a symmetric $(SI)_n$ copolymer is capable of assuming upon microphase separation is given by $2^{2(n-1)}$, indicating that the area density of junction sites per molecule within a given interphase region becomes increasingly more sensitive to molecular conformation (i.e., block looping) as n increases. A fully extended, or bridged, molecule with no looped blocks, for instance, spans $2n - 1$ different interphases, and each junction resides in a different interphase. If the molecule is fully looped, however, one interphase contains all $2n - 1$ junctions, as seen in Figure 2 for a tetrablock copolymer. Simulations have revealed that, in the most probable conformation, a linear multiblock molecule with $n > 1$ traverses $2(n - 1)^{1/2}$ interphases.[15]

In the present work, several $(SI)_n$ multiblock copolymers (with $n > 1$) are blended with hPS at conditions which favor formation of the OBDD morphology in $(SI)_1$/hPS blends. The objectives here are to (i) identify, by TEM, the morphologies which are generated in these $(SI)_n$/hPS blends and (ii) relate the observed morphologies to copolymer architecture.

Table I. Characteristics of the Linear $(SI)_n$ Multiblock Copolymers and Their Blends[a]

series	designation	n	$M \times 10^{-3}$	$M_S \times 10^{-3}$	$M_{hPS} \times 10^{-3}$	M_{hPS}/M_S
CLCs	$(SI)_2$/hPS15	2	120	30	15	0.50
	$(SI)_3$/hPS10	3	120	20	10	0.50
	$(SI)_4$/hPS7	4	120	15	6.5	0.43
VLCs	$(SI)'_2$/hPS7	2	72	18	6.5	0.36
	$(SI)'_3$/hPS7	3	108	18	6.5	0.36

[a] M, M_S, and M_{hPS} denote the molecular weights of the copolymer, styrene block, and homopolymer, respectively. The volume fraction of styrene in each blend is 66 vol %.

Experimental Section

Materials. Two series of perfectly-alternating linear $(SI)_n$ multiblock copolymers were synthesized via anionic polymerization in cyclohexane at 60 °C, with *sec*-butyllithium as the initiator.[13] In accord with previous work,[14] the copolymers possessing constant total molecular weight are referred to here as constant-length copolymers (CLCs), whereas the materials with constant block length are denoted variable-length copolymers (VLCs). The composition of each copolymer was verified with proton nuclear magnetic resonance (^{1}H NMR), using a General Electric QE-300 spectrometer operated at 300 MHz. Block and total molecular weights were determined from gel permeation chromatography (GPC), performed with Waters Ultrastyragel columns of 50-, 100-, 1000-, and 10 000-nm porosities. Typical polydispersity indices were less than 1.09. The molecular characteristics and designations of these materials are given in Table I. Three polystyrene homopolymers were also synthesized, with polydispersity indices of less than 1.03 (as determined by GPC). They are designated here as hPS*M*, where *M* is the number-average molecular weight multiplied by 10^{-3} and rounded to the nearest integral value.

Methods. Concentrated (5% w/v) solutions of these blends were prepared by dissolving predetermined quantities of each copolymer and corresponding homopolymer in reagent-grade toluene. The characteristics of these blends are also provided in Table I. Since these copolymers dissolve more slowly than their diblock analogs, the solutions were allowed to equilibrate overnight (ca. 15 h) and then cast into Teflon molds. Films measuring about 3 mm thick were obtained through solvent evaporation over the course of 3 weeks (unless otherwise indicated) in a toluene-rich environment. The resultant films were heated to 50–70 °C for 1 day, followed by 90–100 °C (under partial vacuum) the second day. They were subsequently encapsulated in glass tubes, subjected to high vacuum, cycled with Ar three times, and then sealed under an Ar atmosphere for a 1-week anneal at 165 °C. No signs of gross oxidative degradation resulted, since no color change occurred and the annealed films readily redissolved in toluene.

Bulk films were sectioned at −100 °C using a Diatome 35° cryodiamond knife on a Reichert-Jung FC-4E ultramicrotome to produce electron-transparent specimens measuring about 70 nm thick. To avoid surface effects arising from preferential enrichment/migration,[16] only the middle of each bulk film was sectioned. The unsaturated isoprene-rich microdomains in these specimens were preferentially stained for 90 min with OsO_4 vapor from a 2% aqueous solution. Electron micrographs were obtained on a Zeiss EM902 electron microscope, operated at 80 keV and an energy loss (ΔE) of 50 eV.

Results and Discussion

Electron micrographs of blends containing the diblock copolymers $(SI)_1$ and $(SI)'_1$ (block lengths of 60 000 and 15 000, respectively) at 66 vol % styrene have been presented elsewhere[6] and are not reproduced here. Suffice it to say that the $(SI)_1$/hPS30 blend exhibits coexisting bicontinuous and cylindrical morphologies, the latter presumably reflecting hPS entanglement, whereas an interconnected lamellar (catenoid) morphology is found in the $(SI)'_1$/hPS7 blend. The OBDD morphology is

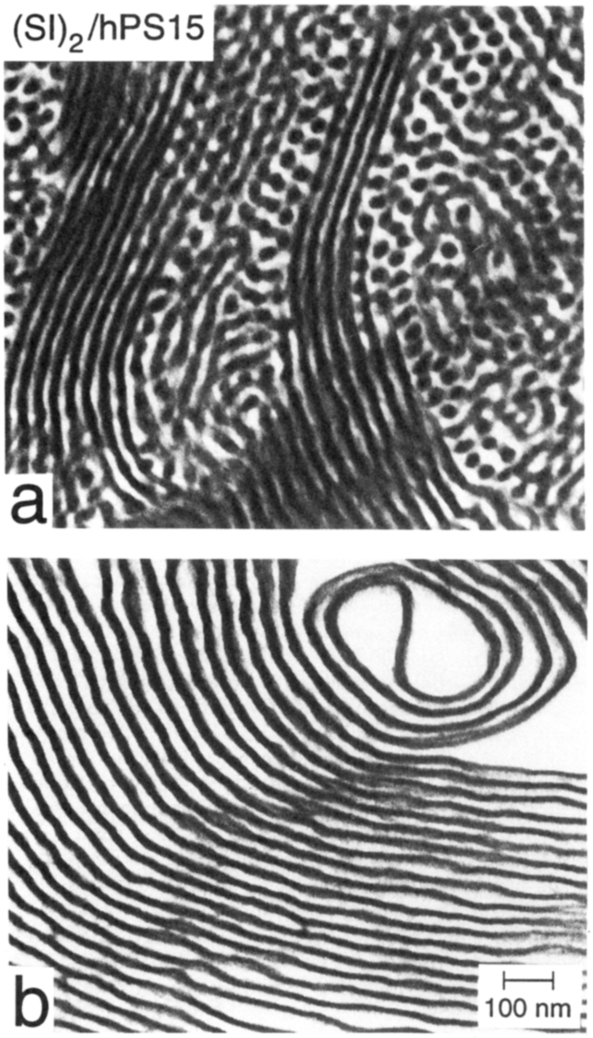

Figure 3. A pair of electron micrographs obtained from the $(SI)_2$/hPS15 blend. The isoprene cylinders in (a) result when the solvent is removed in 3 days. If the blend is dried over the course of 3 weeks, the morphology generated (b) consists of a swollen lamellar copolymer phase and macrophase-separated hPS.

reproducibly observed[6] in binary blends composed of an SI copolymer with a total molecular weight (M) between 20 000 and 80 000 and hPS possessing a molecular weight equal to approximately half that of the styrene block (M/4). Figure 1, for instance, corresponds to a blend consisting of a symmetric copolymer with $M = 60\,000$ and hPS with a molecular weight of 15 000. The inset shown in Figure 1 reveals the same morphology (at higher magnification) in an $(SI)'_1$/hPS3 blend. If the sequential diblock approximation (SDA)[14] is invoked, an $(SI)_n$ multiblock copolymer can be construed as a series of n connected diblock copolymers of reduced molecular weight. The resulting SDA-equivalent molecular weight of a multiblock copolymer is simply M/n and, for the materials studied here, is comparable to that of the diblock copolymers capable of forming the OBDD morphology in copolymer/homopolymer blends.

Electron micrographs of the $(SI)_2$/hPS15 blend are shown in Figure 3. When subjected to solvent evaporation over the course of 3 days, the blend exhibits a morphology comprised primarily of dispersed, and randomly oriented, isoprene cylinders (Figure 3a). While some of the cylinders appear connected and are perhaps related to the "strut" morphology recently proposed by Hashimoto et al.,[17] this morphology most likely reflects a nonequilibrium microstructure due to the rate of solvent evaporation. If the solvent is removed at a slower rate (over the course of 3 weeks), the resultant morphology is closer to equilibrium and is observed to consist of lamellar microdomains and relatively large pools of hPS (Figure 3b). It is of interest to note that the corresponding diblock/hPS blend (in which the blocks are 30 000 each) exhibits the OBDD microstructure (see Figure 1). Recall that the OBDD morphology exists between the cylindrical and lamellar morphologies on the diblock copolymer phase diagram.

Comparison of micrographs (a) and (b) of Figure 3 demonstrates that the morphologies in multiblock copolymer blends are sensitive to the rate of solvent evaporation, a feature which is generally true for block copolymers and their blends.[18] In multiblock copolymer systems, though, the rate of solvent evaporation is deemed particularly important since the interconnected blocks can organize into, and become trapped in, various nonequilibrium or metastable structures. He et al.[19] have shown, for example, that multiblock copolymers composed of poly(dimethylsiloxane) flexible blocks and poly[1-(dimethylsilyl)-4-(dimethylvinylsilyl)benzene] crystallizable blocks tend to gel when rapidly quenched from solution. The physical cross-links in the gel are attributed to aggregates of the incompatible blocks. While a 3-day drying period is presumed to be sufficiently long to achieve near-equilibrium, the $(SI)_2$ copolymer with only four blocks readily self-assembles into cylinders rather than into lamellae. In this case, the hPS is more successful in penetrating into the copolymer and increasing the mean curvature of the microdomain interphase.[4] The morphology produced from slower evaporation is, however, expected to be closer to thermodynamic equilibrium, suggesting that the copolymer in this blend prefers to self-organize without incorporating all of the low-molecular-weight hPS. Although the solubility of hPS within the $(SI)_2$ lamellae is less than that within a diblock copolymer, it is present in sufficient quantity to swell some of the styrene lamellae seen in Figure 3b.

The morphology seen in the $(SI)_3$/hPS10 blend is similar to that presented in Figure 3b for the $(SI)_2$/hPS15 blend and consists of hPS macrophases dispersed in a copolymer matrix. The hPS appears as discrete dispersions in these macrophase-separated blends, since it constitutes the minor blend component (38 wt % added hPS to generate $\Phi_S = 0.66$). An enlargement of the lamellar matrix is shown in Figure 4 and clearly reveals that the copolymer again prefers to exclude, to a significant extent, the hPS. Significant swelling of the styrene microdomains is detected, since the lamellar periodicity (D) obtained from images such as the one in Figure 4 is approximately 27 nm, which is noticeably larger (by $\approx 40\%$) than that of the neat copolymer.[13]

Small dispersed regions of hPS, measuring up to about 200 nm across, are also observed to reside within the lamellae in Figure 4. Recent results obtained by Pan et al.[20] with Monte Carlo simulations and TEM have demonstrated that the addition of small quantities (ca. 10%) of high-molecular-weight hPS to a nearly symmetric poly(styrene-*b*-methylmethacrylate) [P(S-*b*-MMA)] diblock copolymer can result in the formation of hPS aggregates dispersed within an ordered lamellar microstructure. This predicted/observed phenomenon is interpreted in terms of a metastable state that arises due to competition between *micro*phase and *macro*phase separation. Lamellar ordering traps long hPS molecules before they can diffuse to form a separate phase and forces the insoluble hPS to aggregate in order to minimize interfacial contact with

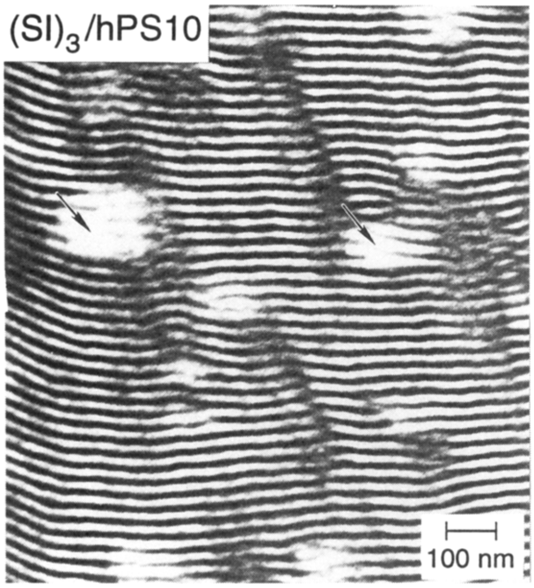

Figure 4. Image of the $(SI)_3$/hPS10 blend showing the lamellar morphology in the microphase-separated copolymer matrix, along with dispersed pools of hPS (arrows). While large hPS regions are observed in this blend, indicating macrophase separation, the hPS dispersions seen here are small aggregates residing within the lamellar network.

the copolymer. Significant exclusion of low-molecular-weight hPS from the lamellar morphology in the present $(SI)_3$/hPS10 blend (discussed further below) suggests that the hPS dispersions seen in Figure 4 may in fact be related to those formed by high-molecular-weight hPS in copolymer-rich P(S-*b*-MMA)/hPS blends.

Blends of a symmetric diblock or triblock copolymer and a parent homopolymer of higher molecular weight than that of the corresponding block in the copolymer are typically macrophase-separated,[5,21] and the lamellae lying near the surface of the copolymer phase tend to orient parallel to the surface as a means of bringing like monomer species into intimate contact and consequently minimizing the free energy. In the $(SI)_3$/hPS10 blend, however, the hPS is of sufficiently low molecular weight to be incorporated within the styrene lamellae. While macrophase-separated domains constitute the chief component of this blend, the high-magnification image of the boundary between copolymer and homopolymer shown in Figure 5 illustrates an interesting feature: the lamellae are oriented normal to the hPS phase. Furthermore, some of the hPS10 effectively solubilizes these lamellae, producing a variety of micellar structures[22-24] which extend into the hPS phase.

Some of the micelles in Figure 5 are connected to the ordered lamellae, while others appear to be isolated within the hPS. (The isolated micelles may have been physically connected to lamellae which were oriented normal to the plane of Figure 5 prior to sectioning, depending on the intersection of this two-dimensional plane with the curved interphase between $(SI)_3$ and hPS10.) While Figure 5 shows a cross-sectioned region across an hPS macrophase, the region presented in Figure 6 intersects an hPS dispersion closer to the copolymer/homopolymer interphase (which, in this case, extends out of the image) and reveals a more highly concentrated micellar network and evidence of organized structure.

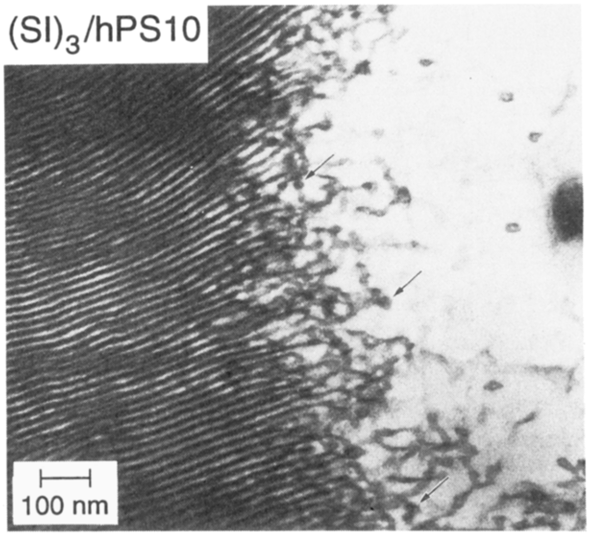

Figure 5. Micrograph of the $(SI)_3$/hPS10 blend revealing hPS solubilization within the copolymer lamellae and disordered block copolymer micelles near the diffuse copolymer/homopolymer interphase. The neighboring lamellae appear to be oriented normal, not parallel, to this interphase. Note that some of the copolymer aggregates remain connected to the lamellae (arrows), while others appear to be isolated within the hPS.

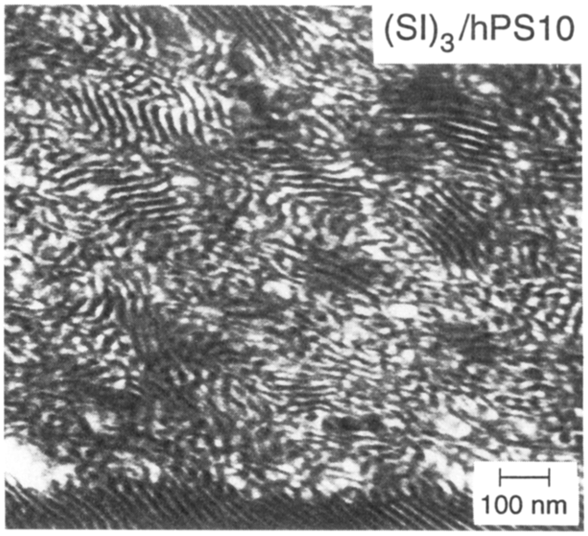

Figure 6. Similar to Figure 5, this image is obtained from the $(SI)_3$/hPS10 blend and shows a region which is cross-sectioned relatively close to the copolymer/homopolymer interphase. Various assembled structures, along with some ordered lamellae, are evident in this micrograph.

As *n* increases in this set of CLCs, the driving force for microphase separation in the copolymer is predicted[14] to decrease. The macrophase separation seen in Figures 3b and 5 is attributed to (i) sufficient driving force for microphase separation in the $(SI)_2$ and $(SI)_3$ copolymers and (ii) the interconnected conformations associated with the multiblock architectures of the copolymers, as illustrated in Figure 7. If microphase separation is strongly favored, the copolymer molecules assume a variety of conformations, from fully extended to fully looped. The chain packing required to accommodate these conformations is presumed to prevent substantial swelling by excluding a significant fraction of the hPS. Thus, exclusion of low-molecular-weight homopolymer in multiblock copolymer blends may present an important consideration in the preparation of commercial blends, such as those composed of segmented polyurethanes.

In essence, the $(SI)_n$/hPS blends investigated here are analogous to solutions which consist of a preferential solvent, and their macrophase-separated morphologies suggest that the copolymers are capable of readily organizing into supramolecular aggregates. Halperin[25] has attempted to address the issue of multiblock copolymer

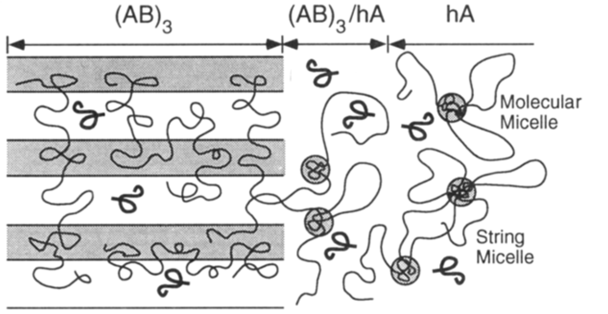

Figure 7. Illustration of the response of a lamellar hexablock copolymer ($n = 3$) to added homopolymer. Within the copolymer phase (denoted as $(AB)_3$), the blocks assume as many as $2^{2(n-1)}$ conformations.[15] Looped blocks would permit lamellar swelling upon homopolymer solubilization, but bridged blocks are presumed to resist such infiltration due to entropic penalties. At the copolymer/homopolymer interphase, $(AB)_3$/hA, the homopolymer and A blocks are in intimate contact, forcing the B blocks to self-assemble into a variety of structures. The B blocks not physically connected to lamellae are presumed to organize into either *molecular* or *string* micelles[25] in the homopolymer (hA) phase. Homopolymer molecules are denoted by darkened lines.

micellization in dilute solutions by invoking scaling relationships for copolymers with highly incompatible blocks. An important feature that he identifies for linear multiblock copolymers is that they can assemble into one of two limiting micellar structures. The *molecular* micelle consists of core and corona regions but is composed of a single copolymer which loops back upon itself $n - 1$ times. *String* micelles arise if discrete micelles are physically linked together via blocks which are compatible with the solvent. Both discrete and connected micellar structures are observed in the micrographs shown in Figures 5 and 6 and depicted in the illustration provided in Figure 7.

As the block lengths of a multiblock copolymer are shortened, however, the incompatibility between the blocks decreases, as does the driving force governing microphase separation in these $(SI)_n$/hPS blends. When hPS is sufficiently incorporated within the styrene microdomains, the free energy of demixing is reduced until microphase separation is no longer favored. In this limit, the discrete microdomains become disordered and all of the isoprene blocks self-assemble into micelles and micelle aggregates to minimize the free energy of the system. This microstructural disorder is seen in Figure 8 for the $(SI)_4$/hPS7 blend and resembles textures produced in low-molecular-weight triblock copolymers[26] and SI/hPS blends.[6] Even though addition of hPS7 disorders the $(SI)_4$ copolymer, Figure 8 reveals that a fraction of homopolymer remains unsolubilized. It is of interest to note that Wang et al.[27] have recently conducted Monte Carlo simulations of symmetric triblock copolymers in a dilute preferential solution and have found that micellization, complete with core and corona regions, occurs only when the blocks are sufficiently incompatible. Otherwise, the molecules aggregate into loose micelles and macrophase-separated gels. The microstructural elements seen in the $(SI)_4$/hPS7 blend (Figure 8) may be related to such gels.

Addition of hPS to the VLCs discussed earlier yields morphologies which differ somewhat from those observed in blends containing the CLCs. The VLC blends provide insight into the influence of block connectivity on blend morphology, since all of the blocks are nominally the same molecular weight (≈15 000).[28] Recall, first, that while the $(SI)'_1$/hPS7 blend was found to exhibit an interconnected lamellar (catenoid-like) morphology, blending $(SI)'_1$ with hPS3 generates the OBDD morphology presented in the inset of Figure 1. Figure 9 is a set of micrographs obtained from the $(SI)'_2$/hPS7 blend. The low-magnification image in Figure 9a reveals that the morphology consists of lamellae interspersed with regions of hPS, reminiscent of the $(SI)_2$/hPS15 blend displayed in Figure 3b. Unlike typical macrophase-separated morphologies, the texture in this micrograph does *not* appear as a dispersion of one phase in a matrix of the other. It does, however, resemble some of the morphologies reported by Löwenhaupt and Hellmann[18] for PMMA/P(S-*b*-MMA) binary blends.

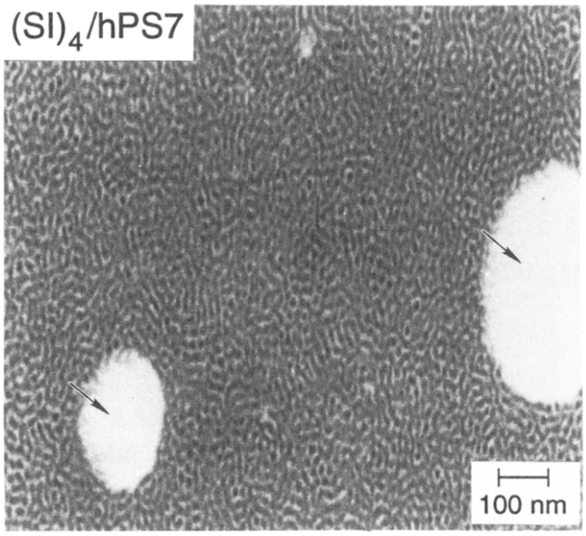

Figure 8. Addition of hPS7 to the $(SI)_4$ copolymer results in complete microstructural disorder, as observed in this micrograph. Isoprene-rich micelles are observed in a styrene matrix, suggesting that the copolymer molecules underwent self-assembly but were unable to develop an ordered network. Macrophase separation, as determined from the presence of hPS dispersions (arrows), is also evident.

The inset provided in Figure 9a is an enlargement of a copolymer "bridge" across an hPS region. This structure corresponds to a thin three-dimensional copolymer membrane separating adjacent hPS macrophases. It spans almost 550 nm in the projection shown in Figure 9a and consists of five discrete layers (three composed of styrene and two of isoprene) which exhibit a periodicity of about 23 nm, thereby indicating that its length is approximately 24 × D. Figure 9b is another enlargement of the $(SI)'_2$/hPS7 blend, this time showing the alternating lamellae in one of the copolymer-rich regions. The value of D estimated from these lamellae is approximately 29 nm, which is in excellent agreement with that of the neat copolymer (as measured with small-angle X-ray scattering).[28] This feature indicates that the styrene microdomains in the lamellar matrix are virtually unaffected by the addition of hPS.

The morphology produced in the $(SI)'_3$/hPS7 blend after solvent evaporation over the course of 3 weeks is similar in appearance to that seen in the $(SI)_2$/hPS15 blend dried relatively quickly (i.e., 3 days) and is not included here for that reason. The third blend in the VLC series is the $(SI)_4$/hPS7 system, previously provided in Figure 8. Comparison of these morphologies reveals that, as n increases, the solubility of hPS within the styrene microdomains of the copolymers is sufficient to induce morphological transitions from lamellae (which are most energetically favored) to isoprene cylinders to disordered micelles. This behavior is in marked contrast with that observed in the blends composed of the CLCs (Figures 3–6 and 8), in which hPS solubilization was minimal and macrophase separation preferred.

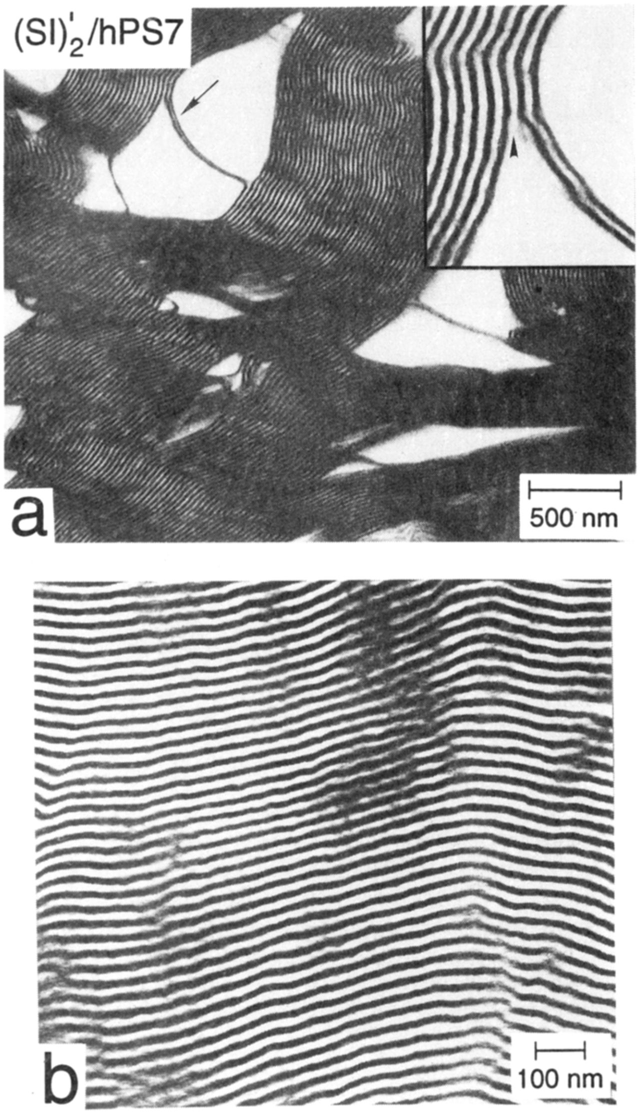

Figure 9. A series of electron micrographs obtained from the (SI)'$_2$/hPS7 blend. A low-magnification image is presented in (a) and reveals the presence of discrete copolymer and hPS-rich regions. Note that the latter do not resemble the spheroidal dispersions often seen in macrophase separation. The inset shown in (a) is an enlargement of a two-dimensional copolymer "bridge", which is a cross-section of a thin five-layer membrane and which is visible in the low-magnification image (arrow). Note that, at the base of the "bridge", one of the styrene lamellae is open to the hPS macrophase (arrowhead). The lamellar network comprising the copolymer phase is shown more clearly in (b).

Morphological variations resulting in these VLC blends are not entirely unexpected, since the neat diblock copolymer (SI)'$_1$ is not far removed from the order–disorder transition (ODT).[6,29] As n increases in either multiblock copolymer series, the driving force for microphase separation is found to decrease, whereas the thickness of the interphase region increases.[30] Blending these copolymers with low-molecular-weight homopolymer reflects this same relationship, indicating that, in addition to factors such as temperature, homopolymer molecular weight, and blend composition,[31] the Flory–Huggins interaction parameter (χ) is dependent on n in multiblock copolymer/homopolymer blends, especially if the neat copolymers are relatively close to the ODT. In fact, the VLC blends reveal that an increase in n alone can promote morphological transitions in these blends when all other molecular and blend parameters are held constant.

The results presented here clealy demonstrate that molecular architecture has a pronounced effect on the observed blend morphologies. Linear (SI)$_n$ multiblock copolymers ($n > 1$) are distinguished from their diblock analogs ($n = 1$) by virtue of the constrained $2(n-1)$ middle blocks. This feature of multiblock copolymers has little impact on the enthalpic contribution to the free energy, but instead dominates the conformational entropy.[15] Winey et al.[4] have shown that morphologies arising in diblock copolymer/homopolymer blends can be correlated with the interphase area occupied by the block junctions. Recall that, in a microphase-separated diblock copolymer, the number of junction sites per molecule residing in a single interphase (κ) is equal to the number of molecules present within the interphase. One may show that, for an (SI)$_n$ molecule, κ is bounded by unity (for all n), if the molecule assumes a bridged conformation (no two junctions in the same interphase), and $2n - 1$, if the molecule is fully looped (all of the junctions reside in a single interphase). An average $\kappa(n)$ lies between these two limits.

The area within the microdomain interphase occupied by a multiblock molecule is therefore dictated by κ. When $n = 1$, $\kappa = 1$ and, subject to the conditions listed earlier, (SI)$_1$/hPS blends are capable of organizing into a bicontinuous morphology in which each molecule is restricted to one interphase. As n is increased to 2, the morphology observed in copolymer/hPS blends consists of lamellae with excluded hPS. In this case, κ varies between 1 and 3 sites/molecule, and the average number of different interphases traversed by an (SI)$_2$ molecule is 2.[15] A dispersed cylindrical, or perhaps strut,[17] morphology which is intermediate to the lamellar and disordered states is observed in the VLC blend when $n = 3$. The interphase area occupied by a single hexablock molecule in this blend also increases and assumes a broadened distribution ($5 \leq \kappa \leq 1$). Isoprene-rich micelles lacking long-range order are found in the (SI)$_4$/hPS7 blend, for which $7 \leq \kappa \leq 1$. Thus, as n increases, the average value and distribution of κ also increases, which, in turn, results in an increase in the occupied interphase area per molecule.

Earlier efforts[4,5] have demonstrated that morphological changes are produced in diblock copolymer/homopolymer blends by increasing the bulk composition of one monomer species (styrene) and, consequently, the interphase area occupied per molecule. The distribution of hPS has also been found to play a crucial role in altering the mean interphase curvature and, hence, morphology. In this work, the bulk composition *and* hPS chain length are held constant and yet a similar trend is observed in the blends composed of VLC copolymers. This behavior reflects an increase in interphase area which is induced solely by the increased number of block junctions in these multiblock copolymer/homopolymer blends. Moreover, the observation that the OBDD morphology is not included in this trend suggests that this bicontinuous microstructure is very sensitive to molecular packing and conformation. Since hPS exclusion is observed in most of the blends presented here, copolymer self-organization is believed to be favored over complete hPS solubilization, thereby resulting in morphologies which may in fact be frozen into metastable states.

Conclusions

The morphologies produced in a series of blends containing well-defined linear (SI)$_n$ multiblock copolymers and homopolystyrene have been investigated here with TEM. The molecular weight of hPS employed in each blend was approximately half that of the styrene blocks in each of the copolymers, and the bulk composition of styrene was maintained at 66 vol % in an effort to produce the OBDD morphology. Blends with copolymers possessing four blocks ($n = 2$) appear to macrophase-separate, generating a lamellar copolymer phase and an hPS-rich phase. This morphology is sensitive to the rate of solvent evaporation. When n is increased to 3, the blends exhibit morphologies between lamellar and disordered textures. In one blend, a lamellar copolymer phase is observed to coexist with an hPS-rich phase. Disordered copolymer micelles are evident at the fringed copolymer/homopolymer interphase. In another, a single dispersed cylindrical morphology is favored. The morphology found in blends composed of the copolymer with the most blocks ($n = 4$) appears to consist of micelles which lack long-range order. This series of morphological transitions has been correlated with the number of block junctions per interphase per molecule and indicates that molecular architecture constitutes an important parameter in the morphological design of multiblock copolymer/homopolymer blends.

Acknowledgment. We are grateful for discussions with Prof. Anna Balazs (University of Pittsburgh), who provided us with a preprint of ref 20. We also thank Mr. M. A. Burchfield for assistance in encapsulating the blends for high-temperature annealing.

References and Notes

(1) Hasegawa, H.; Tanaka, H.; Yamasaki, K.; Hashimoto, T. *Macromolecules* **1987**, *20*, 1651.
(2) Thomas, E. L.; Alward, D. B.; Kinning, D. J.; Martin, D. C.; Handlin, D. L.; Fetters, L. J. *Macromolecules* **1986**, *19*, 2197.
(3) Thomas, E. L.; Anderson, D. M.; Henkee, C. S.; Hoffman, D. *Nature* **1988**, *334*, 598.
(4) Winey, K. I.; Thomas, E. L.; Fetters, L. J. *J. Chem. Phys.* **1991**, *95*, 9367.
(5) Winey, K. I.; Thomas, E. L.; Fetters, L. J. *Macromolecules* **1992**, *25*, 422, 2645.
(6) Spontak, R. J.; Smith, S. D.; Ashraf, A. *Macromolecules* **1993**, *26*, 956.
(7) Spontak, R. J.; Smith, S. D.; Satkowski, M. M.; Ashraf, A. *Macromolecules*, manuscript in preparation.
(8) Herman, D. S.; Kinning, D. J.; Thomas, E. L.; Fetters, L. J. *Macromolecules* **1987**, *20*, 2940.
(9) Anderson, D. M.; Bellare, J.; Hoffman, J. T.; Hoffman, D.; Gunther, J.; Thomas, E. L. *J. Colloid Interface Sci.* **1992**, *148*, 398.
(10) Anderson, D. M.; Davis, H. T.; Scriven, L. E.; Nitsche, J. C. C. *Adv. Chem. Phys.* **1990**, *77*, 337.
(11) Anderson, D. M.; Thomas, E. L. *Macromolecules* **1988**, *21*, 3221.
(12) Wang, Z.-G.; Safran, S. A. *Mater. Res. Soc. Symp. Proc.* **1990**, *177*, 15.
(13) Spontak, R. J.; Smith, S. D.; Satkowski, M. M.; Ashraf, A.; Zielinski, J. M. In *Polymer Solutions, Blends, and Interfaces*; Noda, I., Rubingh, D. N., Eds.; Elsevier: Amsterdam, 1992; pp 65–88.
(14) Zieliński, J. M.; Spontak, R. J. *Macromolecules* **1992**, *25*, 653.
(15) Spontak, R. J.; Zielinski, J. M.; Lipscomb, G. G. *Macromolecules* **1992**, *25*, 6270.
(16) Hariharan, A.; Kumar, S. K.; Russell, T. P. *Macromolecules* **1990**, *23*, 3584; **1991**, *24*, 4909.
(17) Hashimoto, T.; Koizumi, S.; Hasegawa, H.; Izumitani, T.; Hyde, S. T. *Macromolecules* **1992**, *25*, 1433.
(18) Löwenhaupt, B.; Hellmann, G. P. *Polymer* **1991**, *32*, 1065.
(19) He, X.; Herz, J.; Guenet, J. M. *Macromolecules* **1987**, *20*, 2003; **1988**, *21*, 1757; **1989**, *22*, 1390.
(20) Pan, T.; Huang, K.; Balazs, A. C.; Kunz, M. S.; Mayes, A. M.; Russell, T. P. *Macromolecules* **1993**, *26*, 2860.
(21) Quan, X.; Gancarz, I.; Koberstein, J. T.; Wignall, G. D. *Macromolecules* **1987**, *20*, 1434. See also: Quan, X. Ph.D. Thesis, Princeton University, 1986.
(22) Shull, K. R.; Winey, K. I.; Thomas, E. L.; Kramer, E. J. *Macromolecules* **1991**, *24*, 2748.
(23) Kinning, D. J.; Winey, K. I.; Thomas, E. L. *Macromolecules* **1988**, *21*, 3502. Kinning, D. J.; Thomas, E. L. *Macromolecules* **1984**, *17*, 1712.
(24) Nojima, S.; Roe, R.-J.; Rigby, D.; Han, C. C. *Macromolecules* **1990**, *23*, 4305. Rigby, D.; Roe, R.-J. *Macromolecules* **1984**, *17*, 1778; **1986**, *19*, 721. Roe, R.-J. *Macromolecules* **1986**, *19*, 728.
(25) Halperin, A. *Macromolecules* **1991**, *24*, 1418.
(26) Hadziioannou, G.; Skoulios, A. *Macromolecules* **1982**, *15*, 258.
(27) Wang, Y.; Mattice, W. L.; Napper, D. H. *Macromolecules* **1992**, *25*, 4073.
(28) Smith, S. D.; Spontak, R. J.; Satkowski, M. M.; Ashraf, A.; Lin, J. S. *Phys. Rev. B* **1993**, *47*, 14555.
(29) Leibler, L. *Macromolecules* **1980**, *13*, 1602.
(30) Spontak, R. J.; Smith, S. D.; Satkowski, M. M.; Ashraf, A. Presented at the *Polymer* Conference, Cambridge, England, July 1993.
(31) Hashimoto, T.; Tanaka, H.; Iizuka, N. In *Space-Time Organization in Macromolecular Fluids*; Tanaka, F., Doi, M., Ohta, T., Eds; Springer-Verlag: Berlin, 1989.